



THE UNIVERSITY *of* EDINBURGH

Edinburgh Research Explorer

## The effects of polydispersity on the initial susceptibilities of ferrofluids

### Citation for published version:

Camp, PJ, Elfimova, EA & Ivanov, AO 2014, 'The effects of polydispersity on the initial susceptibilities of ferrofluids', *Journal of Physics: Condensed Matter*, vol. 26, no. 45, 456002. <https://doi.org/10.1088/0953-8984/26/45/456002>

### Digital Object Identifier (DOI):

[10.1088/0953-8984/26/45/456002](https://doi.org/10.1088/0953-8984/26/45/456002)

### Link:

[Link to publication record in Edinburgh Research Explorer](#)

### Document Version:

Peer reviewed version

### Published In:

Journal of Physics: Condensed Matter

### General rights

Copyright for the publications made accessible via the Edinburgh Research Explorer is retained by the author(s) and / or other copyright owners and it is a condition of accessing these publications that users recognise and abide by the legal requirements associated with these rights.

### Take down policy

The University of Edinburgh has made every reasonable effort to ensure that Edinburgh Research Explorer content complies with UK legislation. If you believe that the public display of this file breaches copyright please contact [openaccess@ed.ac.uk](mailto:openaccess@ed.ac.uk) providing details, and we will remove access to the work immediately and investigate your claim.



# The effects of polydispersity on the initial susceptibilities of ferrofluids

Philip J. Camp<sup>1‡</sup>, Ekaterina A. Elfimova<sup>2</sup>, and Alexey O. Ivanov<sup>2</sup>

<sup>1</sup>School of Chemistry, University of Edinburgh, West Mains Road, Edinburgh EH9 3JJ, Scotland

<sup>2</sup>Institute of Mathematics and Computer Sciences, Ural Federal University, 51 Lenin Avenue, Ekaterinburg 620000, Russia

E-mail: philip.camp@ed.ac.uk, ekaterina.elfimova@urfu.ru, alexey.ivanov@urfu.ru

4<sup>th</sup> September 2014

**Abstract.** The effects of particle-size polydispersity on the initial susceptibilities of concentrated ferrofluids are analyzed using a combination of theory and computer simulation. The study is focused on a model ferrofluid with a prescribed magnetic-core diameter distribution, a fixed non-magnetic surface layer (corresponding to a demagnetized layer and adsorbed surfactant), and a combination of dipolar and hard-core interactions. The non-trivial effects of polydispersity are identified by comparing the initial susceptibilities of monodisperse and polydisperse ferrofluids with the same Langevin susceptibility. The theory is based on a correction to the second-order modified mean-field theory arising from a formal Mayer-type cluster expansion; this correction is dependent on a parameter similar to the normal dipolar coupling constant, except that it contains a complicated double average over the particle-size distribution, which means that the initial susceptibility should depend significantly on polydispersity. Specifically, the theory predicts that the initial susceptibility is enhanced significantly by polydispersity. This prediction is tested rigorously against results from Monte Carlo simulations, and is found to be robust. The qualitative agreement between theory and simulation is already satisfactory, but the quantitative agreement could be improved by a systematic extension of the cluster expansion. The overall conclusion is that polydispersity should be accounted for carefully in magnetogranulometric analyses of real ferrofluids.

*Keywords:* Ferrofluids, polydispersity, magnetic susceptibility, theory, simulation

‡ Corresponding author: philip.camp@ed.ac.uk

## 1. Introduction

Ferrofluids are colloidal suspensions of magnetized, roughly spherical nanoparticles in an inert carrier liquid [1]. There are three main types of ferrofluid. In ionic aqueous ferrofluids the particles are charge stabilized, and the repulsive electrostatic interactions between them can be controlled by added salt. A second class of aqueous ferrofluids is stabilized by a combination of steric and electrostatic effects. In this case, the particles are surface-functionalized with molecules containing ionizable groups, and so the balance of steric and electrostatic stabilization can be controlled by factors such as pH. In the third and most common class of ferrofluids, the particles are suspended in a non-aqueous medium such as kerosene or mineral oil, and are sterically stabilized by adsorbed polar surfactant molecules such as oleic acid. There are many synthetic routes to such materials [2], but the ultimate goal is to produce suspensions of particles with prescribed sizes and shapes.

Denoting the magnetic-core diameter by  $x$ , and the total thickness of the non-magnetic surfactant layer and demagnetized particle-surface layer by  $\delta/2$ , the effective hard-core diameter of a particle is given by

$$\sigma = x + \delta. \quad (1)$$

The diameters of the magnetic cores are typically on the 1–10 nm scale, but they are rarely uniform within a given sample, leading to considerable particle-size polydispersity. Particle-size distributions can be estimated directly with microscopy techniques, although this is a time-consuming approach, and subject to sampling errors. An alternative approach is to analyze magnetic properties such as the magnetization curve  $M(H)$ , where  $M$  and  $H$  are the magnetization and external magnetic field, respectively, or the initial susceptibility  $\chi$ , which largely dictates the magnetization curve. In this approach, a theory for the magnetic properties of a model ferrofluid of arbitrary polydispersity is parameterized and then fitted to the measured experimental data. In many cases, the particles are modelled as hard spheres with embedded point dipoles – dipolar hard spheres (DHSs). The choice of internally fixed or fluctuating dipoles does not affect the equilibrium thermodynamic and structural properties, but it should be borne in mind that the dynamical properties do depend on whether the dipoles relax by Brownian rotation of the particles or Néel rotation within the particles [1]. There are many theories that account for the short-range interactions and the long-range magnetic dipolar interactions between the particles, and their effects on the bulk magnetic properties of the ferrofluid. These include the original Langevin theory for non-interacting particles [3], the mean-field model of Weiss [4, 5], the mean-spherical approximation (MSA) closure of the Ornstein-Zernike equation [6, 7], thermodynamic perturbation theories [8, 9], so-called modified mean-field models [10, 11], Mayer-type cluster expansions [12, 13, 14], and density functional theory (DFT) [15, 16, 17]. Some of these theories are related. The first-order modified mean-field (MMF1) theory of Pshenichnikov *et al.* was derived from the original Weiss mean-field model on the assumption that the effective field inside the ferrofluid is linearly dependent on the

Langevin magnetization [10]; the results coincide with the first-order high-temperature approximation (HTA) [8, 9]. The MMF2 theory is based on a higher-order temperature expansion [11], but the results are similar in form to the MMF1 theory, hence the MMF2 designation.

Some details should be noted before proceeding with this introduction. The most important physical parameters of the ferrofluid are the particle concentration and the strength of the dipolar interactions. These are characterized by the following properties. Within the DHS model, the hard-core volume fraction  $\varphi_v$  and the magnetic-core volume fraction  $\varphi_m$  are defined by

$$\varphi_v = \frac{\pi}{6} \frac{N \langle \sigma^3 \rangle}{V} = \frac{\pi}{6} \rho \langle \sigma^3 \rangle \quad (2)$$

$$\varphi_m = \frac{\pi}{6} \frac{N \langle x^3 \rangle}{V} = \frac{\pi}{6} \rho \langle x^3 \rangle \quad (3)$$

where  $N$  is the total number of particles,  $V$  is the system volume,  $\rho = N/V$  is the number concentration, and  $\langle \dots \rangle$  denotes an average over the magnetic-core diameter distribution,  $p(x)$ . The strength of the magnetic interactions is most simply measured by a dipolar coupling constant, one choice for which is

$$\lambda = \frac{\mu_0}{4\pi} \frac{\langle m^2 \rangle}{k_B T \langle \sigma^3 \rangle} \quad (4)$$

where  $\mu_0$  is the magnetic permeability of the vacuum,  $m \propto x^3$  is the particle magnetic dipole moment,  $k_B$  is Boltzmann's constant, and  $T$  is the temperature.

A thorough investigation of the magnetization curves of real and simulated ferrofluids was presented in [18, 19]. In this case, the magnetic particles were modelled theoretically and in Monte Carlo (MC) simulations as dipolar hard spheres. Experimental data were measured for a magnetite ferrofluid sample at  $T = 293$  K diluted to various particle concentrations, so that the particle-size distribution was the same in each case. The dipolar coupling constant had the value  $\lambda \simeq 0.63$ , and in the most-concentrated sample,  $\varphi_v \simeq 0.53$  and  $\varphi_m \simeq 0.12$ . The particle-size distribution was modelled using a  $\Gamma$ -distribution, with two fit parameters. Each of the aforementioned theories (except for DFT, because it was not available at the time) was fitted against the experimental data. Only the second-order modified mean-field (MMF2) theory of Ivanov and Kuznetsova [11] gave an apparent particle-size distribution that was independent of concentration. To consolidate the results, simulations with the fitted particle-size distribution were carried out, and essentially perfect agreement was demonstrated between experiment and MMF2 theory. Recently, Szalai, Dietrich, and co-workers have carried out comprehensive studies of the magnetization curves of polydisperse ferrofluids from DFT and computer simulations, and with encouraging results [15, 16, 17].

The MMF2 theory gives a very simple expression for the initial susceptibility in terms of the Langevin susceptibility

$$\chi_L = \frac{\mu_0 \rho \langle m^2 \rangle}{3k_B T} \quad (5)$$

$$= 8\varphi_v \lambda \quad (6)$$

$$= 8\varphi_m \left( \frac{\mu_0}{4\pi} \frac{\langle m^2 \rangle}{k_B T \langle x^3 \rangle} \right). \quad (7)$$

In fact, the combination of (2) and (6) serves as a justification for the choice of dipolar coupling constant given in (4). The MMF2 result for  $\chi$  is

$$\chi_{\text{MMF2}} = \chi_L \left( 1 + \frac{\chi_L}{3} + \frac{\chi_L^2}{144} \right) \quad (8)$$

In [18, 19], a comparison of simulation results and theory showed that the MMF2 theory performs rather well in predicting the initial susceptibility up to  $\chi \simeq 5.5$ . The upper limit corresponds to the most-concentrated experimental sample, for which  $\chi_L \simeq 2.7$ . Note that many theories give  $\chi$  solely as a function of  $\chi_L$  [4, 5, 6, 7, 8, 9, 10, 11]; hence, they predict no difference between the susceptibilities of monodisperse and polydisperse ferrofluids with the same Langevin susceptibilities. The recent DFT theory of Szalai, Dietrich, and co-workers appears to possess the same property, inasmuch as there is a ‘master curve’ for the initial susceptibility of polydisperse ferrofluids [17].

In earlier simulation work, Wang and Holm studied the initial susceptibilities and magnetization curves of bidisperse ferrofluids in which the small-particle and large-particle dipolar coupling constants were approximately 1.3 and 5.3, respectively [20]. It was found that the MMF2 theory gave adequate results as long as the large-particle volume fraction was less than about 0.02. The deviation between theory and simulation was attributed to the formation of chains by the large particles, which occurred even in zero applied magnetic field, and was enhanced by the presence of a field. The chains possess large instantaneous magnetic moments, which increases the initial susceptibility. In general, chain formation occurs in zero field when the dipolar coupling constant  $\lambda > 4$  [21, 22]. At very low temperatures and concentrations ring formation can take place [23, 24]. In most real ferrofluids, though, the initial susceptibility is not strongly influenced by such phenomena. In the presence of a field and with strong enough interparticle interactions, chains can dominate the structure of the ferrofluid [25, 26, 27, 28, 29] and then due account must be taken of them in order to describe the full magnetization curve.

Recently, concentrated ferrofluids synthesized by the Perm group have been shown to exhibit immense values of  $\chi \simeq 120\text{--}150$  at temperatures down to  $T \sim 200$  K [30, 31, 32]. These materials have very high magnetic-core volume fractions of up to  $\varphi_m \simeq 0.23$ , and are expected to have dipolar coupling constants  $\lambda \sim 2$ . This poses a very serious problem: what theory is capable of describing the magnetic properties arising from such strongly interacting polydisperse particles? Certainly, the MMF2 theory (and comparable theories) will not be able to predict such high values of  $\chi$ . The Perm group has shown that with the appropriate value of  $\chi_L$  (which can be determined at very low concentrations or at high temperatures, where interparticle correlations are negligible) the MMF2 is inadequate. In the case of monodisperse ferrofluids, (8) can be extended to include (non-vanishing) corrections of order  $\lambda^{2n}$ , where  $n = 1, 2, 3, \dots$ . The details will be discussed below. The evaluation of these corrections for *real* concentrated ferrofluids with particle-size polydispersity has only recently been outlined [33]. It turns out that

the parameter  $\lambda$  should be replaced by a different parameter, denoted  $\Lambda$ , which contains a complicated double average over the particle-size distribution. For realistic models of ferrofluids, the values of these parameters can differ by as much as a factor of 3. In [33], the corrected theory was tested against experimental data for a real concentrated ferrofluid with  $\chi \simeq 120$  at low temperatures, and excellent agreement was achieved.

The purpose of the current work is to carry out a systematic comparison of theory and simulation results for the initial susceptibilities of model monodisperse and polydisperse concentrated ferrofluids with equal values of the Langevin susceptibility ( $0 \leq \chi_L \leq 10$ ) or the dipolar coupling constant ( $0 \leq \lambda \leq 3$ ), and over a range of concentrations ( $0.20 \leq \varphi_v \leq 0.50$ ). In this way, the effects of particle polydispersity on the initial susceptibility can be isolated. These effects are shown to be considerable, accounting for a difference of up to  $\sim 10$  between the monodisperse and polydisperse ferrofluids. The MMF2 theory and similar theories expressing  $\chi$  solely as a function of  $\chi_L$  predict that that polydispersity has no effect on the results. The extended theory is seen to be improved by replacing  $\lambda$  (monodisperse) with  $\Lambda$  (polydisperse), and the trends observed in the simulation results are captured faithfully by the theory.

This article is organized as follows. In section 2, the microscopic model, theoretical expressions, and simulation methods are summarized. The results are presented in section 3, affording a direct comparison of theory and simulation. Section 4 concludes the article.

## 2. Model and methods

The magnetic particles are modelled as dipolar hard spheres, interacting via the pair potential

$$u(\mathbf{r}_{ij}, \mathbf{m}_i, \mathbf{m}_j) = \begin{cases} \infty & r_{ij} < \sigma_{ij} \\ \frac{\mu_0}{4\pi} \left[ \frac{(\mathbf{m}_i \cdot \mathbf{m}_j)}{r_{ij}^3} - \frac{3(\mathbf{m}_i \cdot \mathbf{r}_{ij})(\mathbf{m}_j \cdot \mathbf{r}_{ij})}{r_{ij}^5} \right] & r_{ij} \geq \sigma_{ij} \end{cases} \quad (9)$$

where  $\mathbf{r}_{ij}$  is the interparticle separation vector,  $r_{ij} = |\mathbf{r}_{ij}|$ ,  $\sigma_{ij} = (\sigma_i + \sigma_j)/2$ , and  $\mathbf{m}_i$  is the magnetic dipole moment on particle  $i$ .

### 2.1. Particle distributions

Each system is defined by the magnetic-core diameter distribution,  $p(x)$ . Normally, log-normal or  $\Gamma$ -distributions are chosen as accurate representations of real particle-size distributions. This can cause problems in computer simulations, however, since the distribution has to be discretized in some way, and the large- $x$  tail may not be represented accurately by a small number of particles in the simulation configuration – a small fraction of large particles can still make a significant contribution to the initial susceptibility. In previous work [18, 19] the discretized particle configuration was chosen so that all relevant moments of the distribution matched those of the target continuous

distribution. Formal criteria exist for choosing the number of distinct fractions within a configuration of a number of particles [34].

Here, very simple particle-size distributions are studied in order to eliminate any spurious deviations between theory and simulations related to discretization and finite-size samples. These distributions are either monodisperse, or are polydisperse and consist of four fractions with particle numbers and magnetic-core diameters in the ratios  $150 : 200 : 100 : 50$  and  $0.6 : 1.0 : 1.4 : 1.8$ , respectively. In the simulations of the polydisperse systems, a total of  $N = 500$  particles was used, and the distributions are discussed below with this number of particles. The polydispersity of the distribution can be characterized by the relative width

$$s = \frac{\sqrt{\langle x^2 \rangle - \langle x \rangle^2}}{\langle x \rangle} \quad (10)$$

which gives  $s \simeq 0.363$ . The discrete distribution is a crude representation of a  $\Gamma$ -distribution,  $p(x) = x^\alpha \exp(-x/y)/[y^{\alpha+1}\Gamma(\alpha+1)]$ . The polydispersity of the  $\Gamma$ -distribution is given by  $s = (1+\alpha)^{-1/2}$ . Figure 1 shows a plot of the discrete distribution (in arbitrary units), and the  $\Gamma$ -distribution with the same polydispersity and the same mean  $\langle x \rangle = (\alpha+1)y = 1.04$ , corresponding to  $\alpha \simeq 6.60$  and  $y \simeq 0.137$ . This value of  $\alpha$  is typical for real ferrofluids [18, 19]. It is stressed that the same discretized distribution is used in comparisons between theory and simulation, so that no deviations arise from the choice of particle configuration.

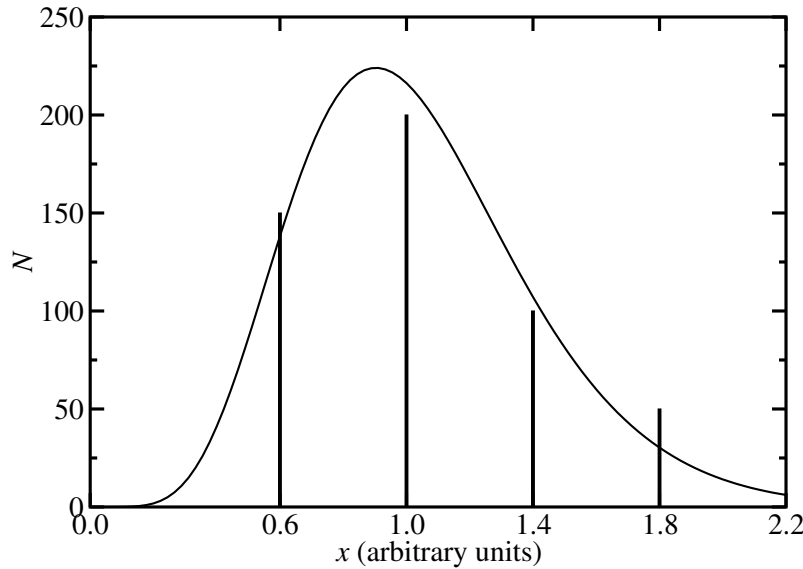


**Figure 1.** The discretized particle-size distribution  $p(x)$  (impulses), and a  $\Gamma$ -distribution with  $\alpha \simeq 6.60$  and  $y \simeq 0.137$  (line). The two distributions have the same polydispersity ( $s \simeq 0.363$ ) and the same mean ( $\langle x \rangle = 1.04$ ).

The effects of polydispersity will be demonstrated either by comparing monodisperse and polydisperse systems with the same hard-core volume fraction  $\varphi_v$ , or the same magnetic-core volume fraction  $\varphi_m$ . Both measures of concentration are

important experimentally:  $\varphi_m$  is determined by the ratio of the saturation magnetization of the ferrofluid to the bulk magnetization of the particle material, while  $\varphi_v$  can either be estimated by assuming the surfactant-layer dimensions, or by fitting small-angle neutron scattering data. The monodisperse system is taken to be a fluid of dipolar hard spheres with magnetic-core diameter  $x_0$ , hard-core diameter  $\sigma_0 = x_0 + \delta$ , and dipole moment  $m_0 \propto x_0^3$ . In this work,  $\delta/x_0 = 1/2$  throughout. In terms of these parameters, the reduced dipole moment  $m_0^*$  and dipolar coupling constant  $\lambda_0$  can be defined as follows.

$$m_0^* = \left( \frac{\mu_0}{4\pi} \frac{m_0^2}{k_B T x_0^3} \right)^{1/2} \quad (11)$$

$$\lambda_0 = \frac{\mu_0}{4\pi} \frac{m_0^2}{k_B T \sigma_0^3} = \frac{(m_0^*)^2}{(1 + \delta/x_0)^3} \quad (12)$$

Comparisons will be made between monodisperse and polydisperse systems with the same Langevin (low-concentration, high-temperature) susceptibility, given by (5)–(7). For a polydisperse system, the reduced dipole moment of fraction  $i$ , and the overall dipolar coupling constant, can be defined just as for the monodisperse system.

$$m_i^* = \left( \frac{\mu_0}{4\pi} \frac{m_i^2}{k_B T x_0^3} \right)^{1/2} \quad (13)$$

$$\lambda = \frac{\langle (m^*)^2 \rangle}{\langle (\sigma/x_0)^3 \rangle} \quad (14)$$

*2.1.1. Equal  $\varphi_v$*  If the monodisperse and polydisperse systems are at the same hard-core volume fraction  $\varphi_v$ , and temperature  $T$ , then the dipolar coupling constants  $\lambda$  (for the polydisperse system) and  $\lambda_0$  (for the monodisperse system) must be equal in order for the systems to have the same  $\chi_L$  (6). Noting that  $\langle m^2 \rangle \propto \langle x^6 \rangle$ , (4) leads to the condition

$$\frac{\langle x^6 \rangle}{\langle \sigma^3 \rangle} = \frac{x_0^6}{\sigma_0^3}. \quad (15)$$

The four-fraction distribution – called  $p_v(x)$  – that satisfies this equal- $\varphi_v$  condition is given in table 1. The reduced dipole moment of each fraction is chosen so that  $\lambda = \lambda_0$ . To give a dipolar coupling constant  $\lambda$ , the reduced dipole moment of fraction  $i$  is

$$m_i^* = \left[ \frac{\lambda \langle (\sigma/x_0)^3 \rangle}{\langle (x/x_0)^6 \rangle} \right]^{1/2} \left( \frac{x_i}{x_0} \right)^3 \quad (16)$$

which satisfies (14). The moments of the distribution are given in table 2, and the reduced dipole moments for  $\lambda = \lambda_0 = 1$  are given in table 1. Tables 1 and 2 show specific quantities corresponding to the monodisperse system with  $\varphi_v = 0.20$ ,  $\lambda_0 = 1.00$ , and  $\chi_L = 1.60$ . Quantities at different concentrations and temperatures can easily be obtained by scaling.



**Table 1.** Magnetic-core diameter distributions for configurations of  $N = 500$  particles:  $N_i$  is the number of particles of fraction  $i$ ;  $x_0$  is the magnetic-core diameter for the monodisperse system;  $x_i$  is the magnetic core diameter;  $\sigma_i = x_i + \delta$  is the hard-core diameter, where  $\delta/x_0 = 1/2$  throughout;  $m_i^*$  is the reduced dipole moment (13) for a system with the same Langevin susceptibility as a monodisperse system with  $\lambda_0 = 1.00$ , and either equal hard-core volume fraction  $\varphi_v$  [ $p_v(x)$ ] or equal magnetic-core volume fraction  $\varphi_m$  [ $p_m(x)$ ].

$i$	$N_i$	$x_i/x_0$	$\sigma_i/x_0$	$m_i^*$
Monodisperse				
0	500	1.000000	1.500000	1.837117
Polydisperse $p_v(x)$				
1	150	0.420266	0.920266	0.136367
2	200	0.700443	1.200443	0.631328
3	100	0.980620	1.480620	1.732363
4	50	1.260797	1.760797	3.681903
Polydisperse $p_m(x)$				
1	150	0.401699	0.901699	0.119080
2	200	0.669498	1.169498	0.551295
3	100	0.937297	1.437297	1.512753
4	50	1.205096	1.705096	3.215151

**Table 2.** System parameters for each of the magnetic-core diameter distributions given in table 1. Parameters for the monodisperse system are given for volume fraction  $\varphi_v = 0.20$ , magnetic-core volume fraction  $\varphi_m = 0.059259$ , and  $\chi_L = 1.60$ , corresponding to  $\lambda_0 = 1.00$ . Parameters are given for polydisperse systems with the same value of  $\chi_L$  and either equal hard-core volume fraction [ $p_v(x)$ ] or equal magnetic-core volume fraction [ $p_m(x)$ ].  $L$  is the simulation box length for a system containing a total of  $N = 500$  particles, as given in table 1. Quantities at different concentrations and temperatures can easily be obtained by scaling.

	Monodisperse	$p_v(x)$	$p_m(x)$
$\langle x^3 \rangle / x_0^3$	1.000000	0.548742	0.479179
$\langle x^6 \rangle / x_0^6$	1.000000	0.628405	0.479179
$\langle \sigma^3 \rangle / x_0^3$	3.375000	2.120866	1.949331
$\langle (m^*)^2 \rangle$	3.375000	2.120866	1.617228
$\lambda$	1.000000	1.000000	0.829632
$\Lambda$	1.000000	1.859723	1.560000
$\varphi_v$	0.200000	0.200000	0.241071
$\varphi_m$	0.059259	0.051747	0.059259
$L/x_0$	16.408573	14.054562	12.840146

**2.1.2. Equal  $\varphi_m$**  If the monodisperse and polydisperse systems are to have the same magnetic-core volume fraction  $\varphi_m$  and Langevin susceptibility  $\chi_L$  at a given temperature

$T$ , then from (7)

$$\frac{\langle x^6 \rangle}{\langle x^3 \rangle} = \frac{x_0^6}{x_0^3}. \quad (17)$$

The four-fraction distribution that satisfies this equal- $\varphi_m$  condition is given in table 1 as  $p_m(x)$ . The reduced dipole moments are chosen so that the right-hand side of (7) is the same for both the monodisperse system (with dipolar coupling constant  $\lambda_0$ ) and the polydisperse system. This leads to

$$m_i^* = \left[ \left( 1 + \frac{\delta}{x_0} \right)^3 \lambda_0 \right]^{1/2} \left( \frac{x_i}{x_0} \right)^3. \quad (18)$$

In this case, the dipolar coupling constants – as defined in (12) and (14) – are not the same in the two systems, since the hard-core volume fractions are not equal either. The values corresponding to monodisperse systems with  $\lambda_0 = 1.00$  are given in table 2. Once again, quantities at different concentrations and temperatures can easily be obtained by scaling.

## 2.2. Theory

For monodisperse systems, a cluster expansion in terms of  $\varphi_v$  and  $\lambda$  leads to a general expression for  $\chi$  of the form

$$\chi = \chi_L + \sum_{k,l=2}^{\infty} B_{kl} \varphi_v^k \lambda^l \quad (19)$$

where  $B_{kl}$  is a virial-type coefficient. Many of the theories mentioned in the Introduction only contain terms with  $k = l$ , giving a formula for  $\chi$  expressed solely in terms of  $\chi_L = 8\varphi_v\lambda$ . For example, the MMF2 expression in (8) corresponds to the inclusion of the exact coefficients  $B_{22} = 64/3$  and  $B_{33} = 32/9$ , and with all others set equal to zero. Huke and Lücke have analyzed the second virial-type coefficients  $B_{2l}$  [12]; only the coefficients with even- $l$  are nonzero. Keeping only  $B_{22}$ ,  $B_{24}$ , and  $B_{33}$  gives [11, 13, 14]

$$\chi_\lambda = \chi_L \left[ 1 + \frac{\chi_L}{3} \left( 1 + \frac{\lambda^2}{25} \right) + \frac{\chi_L^2}{144} \right]. \quad (20)$$

Of course, there is an infinite number of  $\lambda$ -dependent corrections, but they become less significant and more complicated to compute. In a recent magnetogranulometric analysis of the initial susceptibility of a magnetite/linoleic acid ferrofluid, it was found that the first ‘Huke-Lücke’ correction to the MMF2 theory was sufficient to describe the experimental results [35], albeit with  $\lambda$  being determined from the experimental concentration and Langevin susceptibility (6) rather than any microscopic details.

The focus here is on establishing a concrete connection between the microscopic details of the ferrofluid (particle-size distribution, temperature, concentration) and the initial susceptibility. It is tempting to apply (20) to polydisperse systems, simply by

inserting (4) for  $\lambda$ . This is incorrect. The proper extension to the polydisperse case gives the result

$$\chi_\Lambda = \chi_L \left[ 1 + \frac{\chi_L}{3} \left( 1 + \frac{\Lambda^2}{25} \right) + \frac{\chi_L^2}{144} \right] \quad (21)$$

where  $\Lambda$  involves a complicated double average over the particle-size distribution,  $p(x)$  [33]. The explicit expression for  $\Lambda$  in the case of discretized distributions (as defined in section 2.1) is

$$\Lambda = \frac{\mu_0}{4\pi k_B T} \frac{1}{\sum_i N_i m_i^2} \sqrt{\sum_{ij} \frac{N_i N_j m_i^4 m_j^4}{\sigma_{ij}^6}}. \quad (22)$$

Ivanov and Elfimova have shown that for realistic ferrofluid models,  $\Lambda/\lambda$  can be as high as 3 [33]. The result expressed in (21) has been tested against experimental data for a real, high-susceptibility ferrofluid, and excellent agreement has been demonstrated [33]. Obviously, for a monodisperse ferrofluid,  $\Lambda = \lambda = \lambda_0$ . The numerical values of  $\Lambda$  for the equal- $\varphi_v$  and equal- $\varphi_m$  cases with  $\chi_L = 1.60$  are given in table 2. Note that  $\Lambda \geq \lambda$  in all cases.

### 2.3. Computer simulations

Canonical ( $NVT$ ) MC simulations were performed in a cubic simulation box with side  $L$  [36]. For the monodisperse system, the hard-core volume fractions were  $\varphi_v = 0.20$ ,  $0.30$ , and  $0.40$ , representing moderate to high concentrations for real ferrofluids. The dipolar coupling constants were as high as  $\lambda_0 = 3.00$ , which corresponds to very strongly interacting particles. The box dimensions for some monodisperse and polydisperse systems with  $N = 500$  particles and  $\chi_L = 1.60$  are given in table 2. Some other calculations for the monodisperse system were carried out with  $N = 256$  or  $N = 864$  particles. Simulation parameters and results are collected in the Supplementary Data. All calculations were performed in reduced units, defined in terms of the parameters of the monodisperse system, as detailed in section 2.1. The long-range dipolar interactions were computed using the Ewald summation with conducting boundary conditions. Translational and rotational moves of the particles were conducted with maximum displacement parameters giving acceptance rates of 20% and 50%, respectively. Typical run lengths were  $5 \times 10^6$  attempted translations and rotations per particle, after equilibration. The initial susceptibility was determined from the fluctuation formula

$$\chi = \frac{\mu_0 \langle |\mathbf{M}|^2 \rangle}{3k_B T V} \quad (23)$$

where  $\mathbf{M} = \sum_{i=1}^N \mathbf{m}_i$  is the instantaneous dipole moment of the simulation box. The ‘dynamics’ in concentrated systems of strongly interacting particles can be slow, and so the determination of  $\langle |\mathbf{M}|^2 \rangle$  was carried out with some care. Specifically, the probability distributions  $p(M_\alpha)$  ( $\alpha = x, y, z$ ) were plotted and fitted with Gaussian functions in

order to confirm the behaviour expected from the Central Limit Theorem, and therefore that the simulations had been run long enough:

$$p(M_\alpha) = \frac{1}{\sqrt{2\pi B^2}} \exp \left[ -\frac{(M_\alpha - A)^2}{2B^2} \right]. \quad (24)$$

An example is shown in figure 2. These data are for a polydisperse system of  $N = 500$  particles at  $\varphi_v = 0.40$  and with  $1.00 \leq \lambda \leq 2.75$ , where the fluctuations in the instantaneous magnetization are expected to be large. In general, the Gaussian function provides an adequate fit, except in the wings of the distribution where the instantaneous magnetization is approaching its maximum allowed values. In almost all cases, the distributions are centered on  $M_\alpha = 0$ . The one exception is at  $\lambda = 2.75$ , where the strong dipolar interactions lead to long-lived magnetization fluctuations. The apparent net magnetization  $\langle M_\alpha \rangle$  is only a statistical-sampling error. The difference between  $B^2 = \langle M_\alpha^2 \rangle - \langle M_\alpha \rangle^2$  and  $B^2 + A^2 = \langle M_\alpha^2 \rangle$  is less than 0.3% in all cases, and in the majority of cases at least one order of magnitude smaller.  $\chi$  was evaluated by using  $B^2$  as the best estimate of  $\langle |\mathbf{M}|^2 \rangle$  in (23).

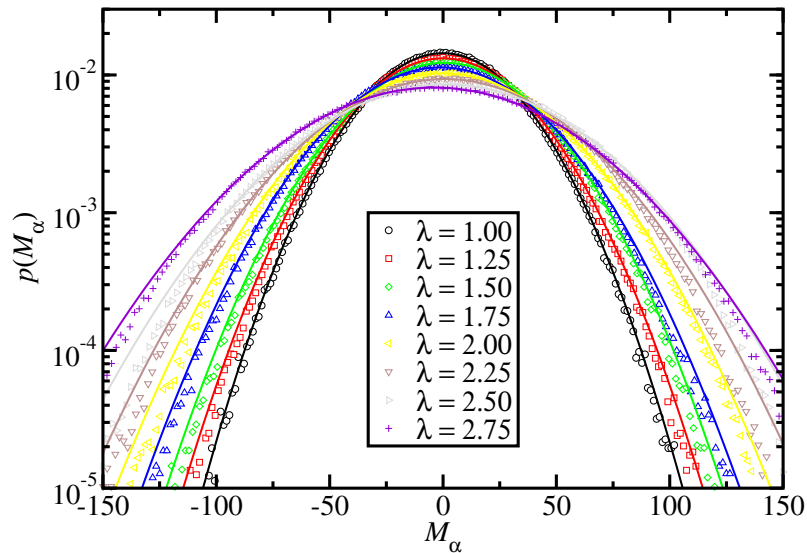


**Figure 2.** Probability distribution of the instantaneous magnetization  $M_\alpha$  (in reduced units) in one direction, from simulations of the polydisperse ferrofluid with  $\varphi_v = 0.40$  and  $1.00 \leq \lambda \leq 2.75$ . The simulation data are shown as symbols, and Gaussian fits are shown with lines.

### 3. Results

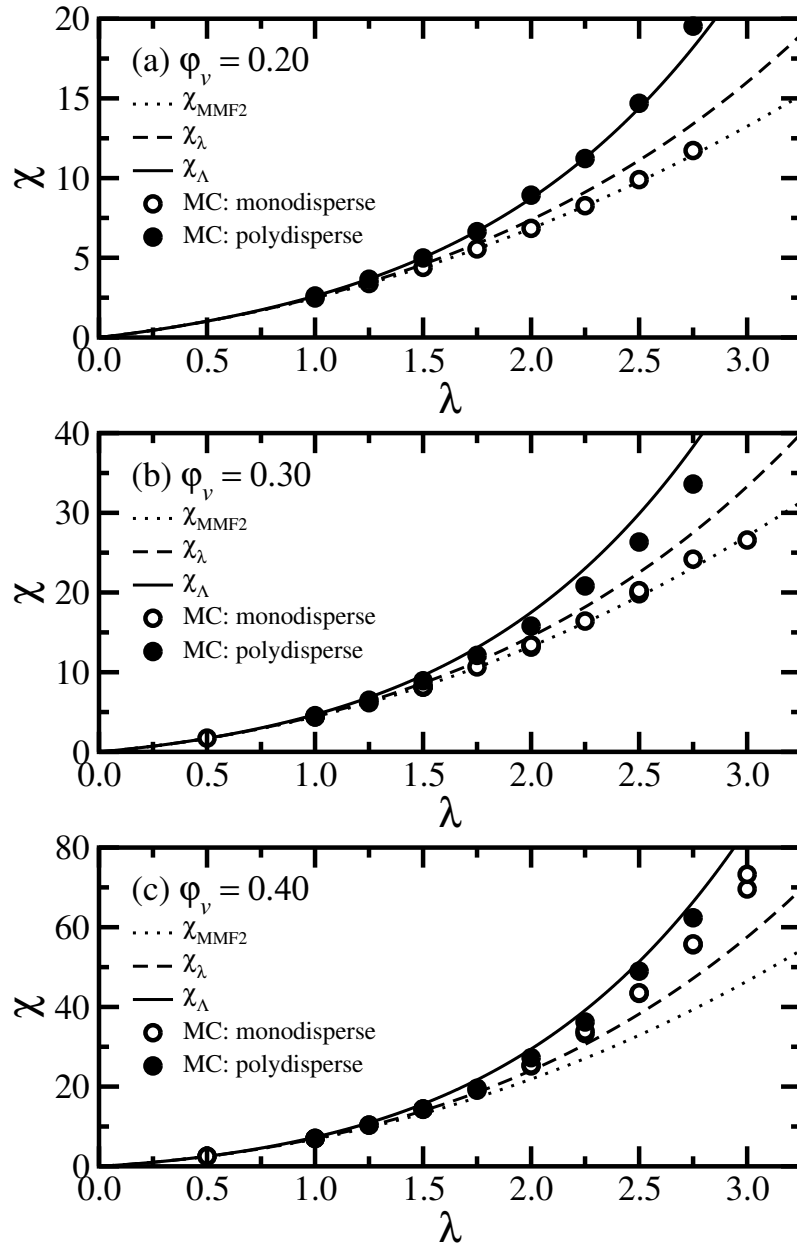
All of the simulation results are collected in the Supplementary Data. In the following plots, simulation results with different system sizes are shown with the same symbols in order to keep the labelling simple. The estimated statistical uncertainties from the fitting procedure described in section 2.3 are reported in the Supplementary Data, but in the plots to follow, they are smaller than the symbol size.

Figure 3 shows  $\chi$  as a function of  $\lambda$  for monodisperse and polydisperse ferrofluids with equal volume fraction  $\varphi_v = 0.20, 0.30$ , and  $0.40$ . Recall from (6) that under these conditions, having the same Langevin susceptibility (5) means having the same value of  $\lambda$  (4). All of the data must fall on to the Langevin line at low concentration and low values of  $\lambda$  (corresponding to high temperature). The simulation results show that, at high values of  $\lambda$ , the susceptibility of the polydisperse ferrofluid is significantly higher than that of the monodisperse ferrofluid. This must be due to there being strong dipolar ‘nose-to-tail’ correlations between the larger particles, leading to larger fluctuations in the instantaneous magnetization. It is not due to the mere presence of large particles with large dipole moments, because the comparison is made between systems with the same Langevin susceptibilities. For polydisperse and monodisperse ferrofluids with  $\lambda = 2.75$  and at  $\varphi_v = 0.20, 0.30$ , and  $0.40$ , the differences in  $\chi$  are 8, 9, and 7, respectively. At  $\varphi_v = 0.40$  and  $\lambda = 3.00$ , the simulation results with different size systems are slightly different, but it’s very difficult to get reliable results with such strongly interacting particles; at lower values of  $\lambda$  and  $\varphi_v$ , there are no finite-size issues.

Figure 3 shows the MMF2 theory, which of course predicts no dependence of  $\chi$  on the polydispersity for systems with the same  $\chi_L$ . The agreement between MMF2 theory and simulation results for the monodisperse system is rather good at  $\varphi_v = 0.20$  and  $0.30$ , but it breaks down at  $\varphi_v = 0.40$ . The extended theory  $\chi_\lambda$  (20) slightly overestimates the monodisperse simulation results at  $\varphi_v = 0.20$  and  $0.30$ , and underestimates them at  $\varphi_v = 0.40$ . Crucially, the polydisperse version  $\chi_\Lambda$  (21) correctly predicts the higher value of  $\chi$  in the polydisperse case. While the simulation results suggest that the difference between  $\chi_\Lambda$  and  $\chi_\lambda$  is roughly independent of volume fraction (being in the range 7–9) the theory predicts a difference that increases with volume fraction. It is not clear what element of the theory causes this deviation, although the fact that the theory is more accurate at low volume fraction suggests that it is to do with truncation of the density expansion in (19). It is stressed that the deviations between theory and simulation are not due to how the distribution is represented in the simulations, because the discretized distribution is used in both theory and simulation. Although the agreement between theory and simulation is not perfect, the fundamental conclusion is that increasing polydispersity significantly increases the initial susceptibility.

Figure 4 shows the corresponding results for monodisperse and polydisperse systems with the same magnetic volume fraction  $\varphi_m$ . The ranges on the  $x$  and  $y$  axes are chosen so that the results for the monodisperse system would overlay those in figure 3, e.g.,  $0 \leq \lambda \leq 3.25$  for  $\varphi_v = 0.20$  in figure 3(a) matches up with  $0 \leq \chi_L \leq 5.2$  in figure 4(a). The simulation results show the same increase in  $\chi$  with polydispersity, but the magnitude of the increase is significantly less than in the equal- $\varphi_v$  case. Table 2 shows that the value of  $\lambda$  is smaller in the equal- $\varphi_m$  case than in the equal- $\varphi_v$  case. Since  $\lambda$  should dictate the extent of dipolar nose-to-tail correlations [37, 38], and hence the magnitude of fluctuations in the instantaneous magnetization, it is to be expected that polydispersity should have less of an influence in the equal- $\varphi_m$  case.

Obviously, the theoretical curves  $\chi_{\text{MMF2}}$  and  $\chi_\lambda$  in figures 3(a)-(c) and 4(a)-(c)



**Figure 3.** Initial susceptibility of monodisperse and polydisperse ferrofluids with equal dipolar coupling constants  $\lambda$  and equal hard-core volume fractions  $\phi_v$ : (a)  $\phi_v = 0.20$ ; (b)  $\phi_v = 0.30$ ; (c)  $\phi_v = 0.40$ . The open symbols are from simulations of the monodisperse system, the filled symbols are from simulations of the polydisperse system, and the dotted, dashed, and solid lines are the expressions  $\chi_{\text{MMF2}}$  (8),  $\chi_\lambda$  (20), and  $\chi_\Lambda$  (21), respectively.

would overlay one another, while  $\chi_\Lambda$  would not. Most importantly,  $\chi_\Lambda$  accurately reflects the reduced influence of polydispersity in the equal- $\phi_m$  case.

Figures 5(a) and (b) show the ratio  $\chi_{\text{poly}}/\chi_{\text{mono}}$  of the initial susceptibilities of polydisperse and monodisperse systems with equal values of  $\phi_v$  and  $\phi_m$ , respectively, from simulations and theory ( $\chi_\Lambda/\chi_\lambda$ ). The fitting errors in  $\chi_\Lambda$  and  $\chi_\lambda$  have been

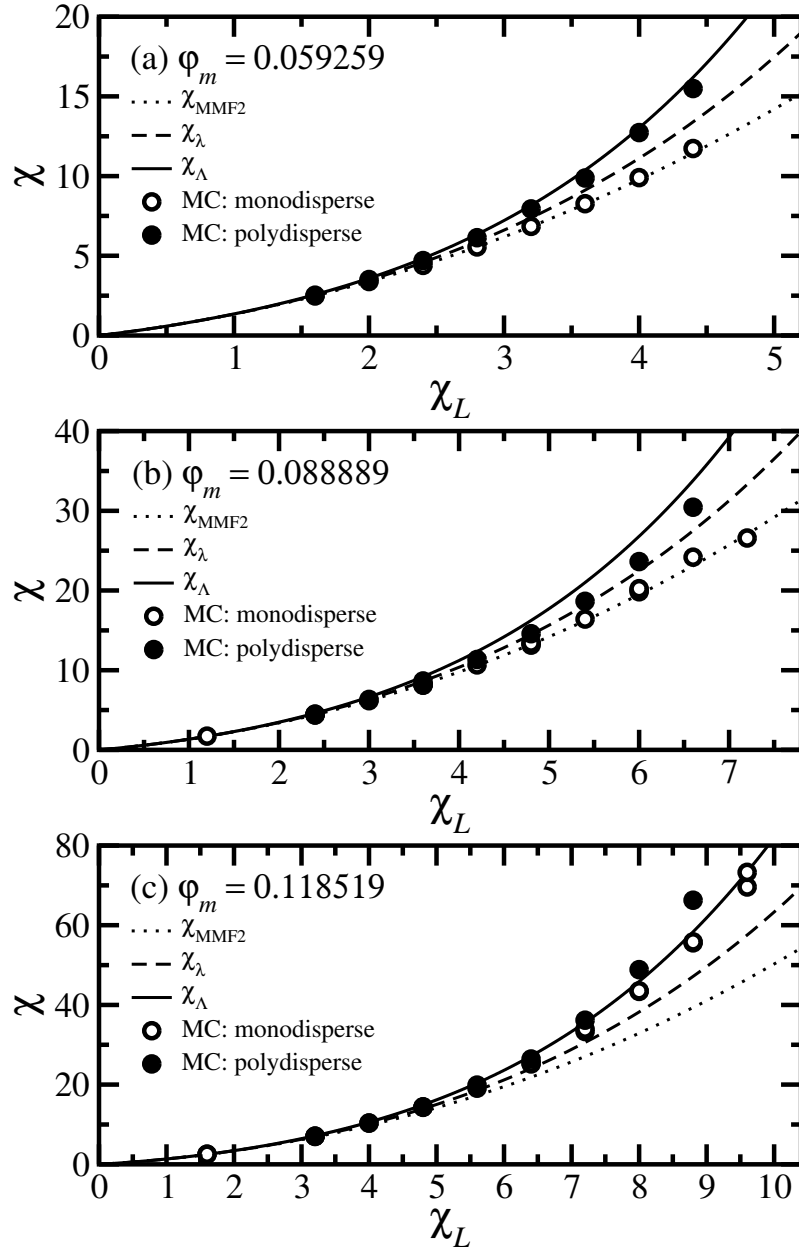


**Figure 4.** Initial susceptibility of monodisperse and polydisperse ferrofluids with equal Langevin susceptibilities  $\chi_L$  and equal magnetic-core volume fractions  $\varphi_m$ : (a)  $\varphi_m = 0.059259$ ; (b)  $\varphi_m = 0.088889$ ; (c)  $\varphi_m = 0.118519$ . The open symbols are from simulations of the monodisperse system, the filled symbols are from simulations of the polydisperse system, and the dotted, dashed, and solid lines are the expressions  $\chi_{\text{MMF2}}$  (8),  $\chi_\lambda$  (20), and  $\chi_\Lambda$  (21), respectively.

propagated here, but they are still smaller than the symbol size; the scatter in the data shows that these uncertainties are underestimates. Note that the MMF2 theory predicts a constant value of  $\chi_{\text{poly}}/\chi_{\text{mono}} = 1$ . Firstly, a comparison of (a) and (b) emphasizes that the enhancement of  $\chi$  by polydispersity is more pronounced in the equal- $\varphi_v$  case; at a moderate volume fraction ( $\varphi_v = 0.20$ ) the enhancement can be very

significant, more than 60% with strongly interacting particles. This effect is significantly reduced in the equal- $\varphi_m$  case. Secondly, the relative enhancement of  $\chi$  decreases with increasing concentration. Finally, the theory does capture the basic dependence of  $\chi$  on polydispersity, but the quantitative agreement with simulation could be improved. The theory underestimates the ratio at low concentration, overestimates it at high concentration, and is accurate at intermediate concentration. As indicated above, this suggests that higher-order terms in the density expansion of (19) may play a role.

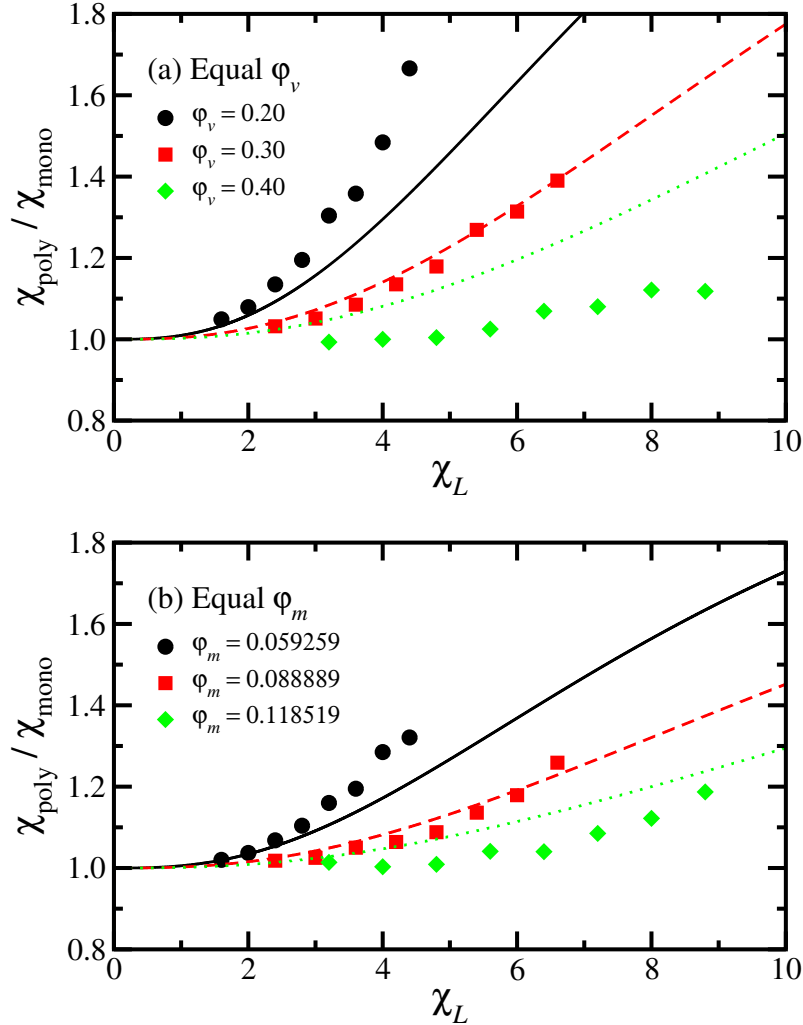


**Figure 5.** Ratio of the initial susceptibilities of polydisperse and monodisperse systems from simulations (points) and theory (lines). The theoretical predictions are given by the ratio of  $\chi_\Lambda$  (21) and  $\chi_\lambda$  (20). In (a), results are shown for  $\varphi_v = 0.20$  (circles and solid line),  $\varphi_v = 0.30$  (squares and dashed line), and  $\varphi_v = 0.40$  (diamonds and dotted line). In (b), results are shown for  $\varphi_m = 0.059259$  (circles and solid line),  $\varphi_m = 0.088889$  (squares and dashed line), and  $\varphi_m = 0.118519$  (diamonds and dotted line).

The results so far concern the discretized particle-size distribution shown in figure 1. The general effects of polydispersity can be characterized by the ratio  $\Lambda/\lambda_0$ ; recall that  $\lambda_0$  is the dipolar coupling constant of the monodisperse system with the same Langevin



susceptibility. This ratio has been calculated for  $\Gamma$ -distributions over a wide range of polydispersity. For a given polydispersity  $s$ , the width parameter for the corresponding  $\Gamma$ -distribution is  $\alpha = s^{-2} - 1$ . To determine the corresponding value of  $y$ , equations (15) and (17) are solved in the equal- $\varphi_v$  and equal- $\varphi_m$  cases, respectively. The non-magnetic layer thickness  $\delta/x_0 = 1/2$  throughout. Figure 6 shows the results for the equal- $\varphi_v$  and equal- $\varphi_m$  cases. Firstly,  $\Lambda$  and  $\lambda$  are larger in the equal- $\varphi_v$  case than in the equal- $\varphi_m$  case. This is just a mathematical consequence of the difference between the two particle-size distributions, arising from the different conditions in equations (15) and (17). Secondly,  $\lambda < \lambda_0$  in the equal- $\varphi_m$  case, again due to the details of the particle-size distribution. The stronger polydispersity effect in the equal- $\varphi_v$  case can therefore be attributed to stronger dipolar correlations, as measured by the coupling constant  $\lambda$ . Finally, table 2 shows that for the discrete distributions,  $\Lambda/\lambda_0 \simeq 1.86$  (equal  $\varphi_v$ ) and 1.56 (equal  $\varphi_m$ ), while figure 6 shows that for the  $\Gamma$ -distribution with the same polydispersity ( $s \simeq 0.363$ ), these ratios are approximately 3.31 and 2.64, respectively. The differences are due to the tails of the  $\Gamma$ -distributions making large contributions to  $\Lambda$ , since equation (22) contains moments of high order.

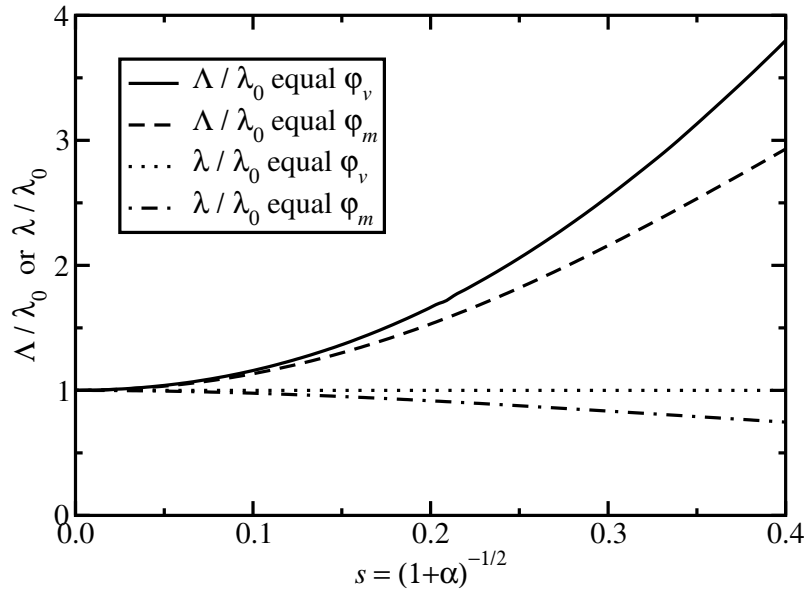


**Figure 6.**  $\Lambda/\lambda_0$  and  $\lambda/\lambda_0$  as functions of polydispersity  $s$  in the equal- $\varphi_v$  and equal- $\varphi_m$  cases. The particle sizes are governed by  $\Gamma$ -distributions for which  $s = (1+\alpha)^{-1/2}$ , and the non-magnetic layer thickness is  $\delta/x_0 = 1/2$  throughout.

#### 4. Conclusions

In this work, the initial susceptibilities of concentrated ferrofluids were examined with a particular focus on the effects of polydispersity. To this end, comparisons were made between model monodisperse and polydisperse systems. The model particles were hard spheres with magnetized cores and a non-magnetic surface layer (mimicking adsorbed

surfactant and demagnetized material). In the polydisperse case, a convenient magnetic-core size distribution was chosen to resemble those for real ferrofluids. Comparisons were made between monodisperse and polydisperse systems with the same Langevin (low-concentration, high-temperature) susceptibility, and either the same hard-core volume fraction or the same magnetic volume fraction. Computer simulations and analytical theory were employed to study the model systems. The theory contained a correct account of the particle-size distribution, and as a result, predicted a difference between the monodisperse and polydisperse cases. A comparison of simulation and theory showed general consistency, inasmuch as polydispersity clearly leads to a significant increase in the initial susceptibility, above and beyond that one would expect merely from the presence of some large particles in the system; this latter, trivial effect is cancelled out by comparing systems with the same Langevin susceptibility. The enhancement of the initial susceptibility is greater at equal hard-core volume fraction than at equal magnetic volume fraction. This is due to the respective values of the dipolar coupling constant in the two cases, and that orientational correlations are expected to be more pronounced in the former case, leading to greater fluctuations in the instantaneous magnetization. Although the quantitative agreement between simulation and theory could be improved, the overall conclusion is unaffected: both approaches show that the particle-size distribution significantly affects the initial susceptibility, and therefore it must be accounted for correctly in theoretical studies and in magnetogranulometric analyses of ferrofluids.

## Acknowledgments

The research was carried out with the financial support of the Ministry of Education and Science of the Russian Federation (Project 3.12.2014/K and Agreement 02.A03.21.0006), and was also partly supported by the Russian Foundation for Basic Research (Grant No. 13-01-96032-r-ural).

## References

- [1] Rosensweig R E 1998 *Ferrohydrodynamics* (New York: Dover Publications, Inc.)
- [2] Laurent S, Forge D, Port M, Roch A, Robic C, Vander Elst L and Muller R N 2008 *Chem. Rev.* **108** 2064–2110
- [3] Langevin P 1905 *J. Phys. Theor. Appl.* **4** 678
- [4] Weiss P 1907 *J. Phys.* **6** 661–690
- [5] Cebers A 1982 *Magnetohydrodynamics* **18**(2) 137–142
- [6] Wertheim M S 1971 *J. Chem. Phys.* **55** 4291–4298
- [7] Morozov K I and Lebedev A V 1990 *J. Mag. Mag. Mater.* **85** 51–53
- [8] Buyevich Yu A and Ivanov A O 1992 *Physica A* **190** 276–294
- [9] Ivanov A O 1992 *Magnetohydrodynamics* **28**(4) 353–359
- [10] Pshenichnikov A F, Mekhonoshin V V and Lebedev A V 1996 *J. Mag. Mag. Mater.* **161** 94–102
- [11] Ivanov A O and Kuznetsova O B 2001 *Phys. Rev. E* **64** 041405
- [12] Huke B and Lücke M 2000 *Phys. Rev. E* **62** 6875–6890
- [13] Huke B and Lücke M 2003 *Phys. Rev. E* **67** 051403

- [14] Huke B and Lücke M 2004 *Rep. Prog. Phys.* **67** 1731–1768
- [15] Szalai I and Dietrich S 2008 *J. Phys.: Condens. Matter* **20** 204122
- [16] Szalai I and Dietrich S 2011 *J. Phys.: Condens. Matter* **23** 326004
- [17] Szalai I, Nagy S and Dietrich S 2013 *J. Phys.: Condens. Matter* **25** 465108
- [18] Ivanov A O, Kantorovich S S, Reznikov E N, Holm C, Pshenichnikov A F, Lebedev A V, Chremos A and Camp P J 2007 *Phys. Rev. E* **75** 061405
- [19] Ivanov A O, Kantorovich S S, Reznikov E N, Holm C, Pshenichnikov A F, Lebedev A V, Chremos A and Camp P J 2007 *Magnetohydrodynamics* **43** 393–400
- [20] Wang Z and Holm C 2003 *Phys. Rev. E* **68** 041401
- [21] Levesque D and Weis J J 1994 *Phys. Rev. E* **49** 5131–5140
- [22] Klokkenburg M, Dullens R P A, Kegel W K, Ern   B H and Philipse A P 2006 *Phys. Rev. Lett.* **96** 037203
- [23] Rovigatti L, Russo J and Sciortino F 2012 *Soft Matter* **8** 6310–6319
- [24] Kantorovich S, Ivanov A O, Rovigatti L, Tavares J M and Sciortino F 2013 *Phys. Rev. Lett.* **110** 148306
- [25] Mendelev V S and Ivanov A O 2004 *Phys. Rev. E* **70** 051502
- [26] Ivanov A O, Kantorovich S S, Mendelev V S and Pyanzina E S 2006 *J. Mag. Mag. Mater.* **300** e206–e209
- [27] Klokkenburg M, Ern   B H, Meeldijk J D, Wiedenmann A, Petushkov A V, Dullens R P A and Philipse A P 2006 *Phys. Rev. Lett.* **97** 185702
- [28] Castro L L, Gon  alves G R R, Skeff Neto K, Morais P C, Bakuzis A F and Miotto R 2008 *Phys. Rev. E* **061507**
- [29] Eloi M T A, Santos, Jr J L, Morais P C and Bakuzis A F 2010 *Phys. Rev. E* **82** 021407
- [30] Pshenichnikov A F and Lebedev A V 2004 *J. Chem. Phys.* **121** 5455–5467
- [31] Pshenichnikov A F and Lebedev A V 2005 *Colloid J.* **67** 189–200
- [32] Lebedev A V 2010 *Colloid J.* **72** 815–819
- [33] Ivanov A O and Elfimova E A 2014 *J. Mag. Mag. Mater.* In press  
URL <http://dx.doi.org/10.1016/j.jmmm.2014.08.067>
- [34] Sturges H A 1926 *J. Am. Stat. Assoc.* **21** 65–66
- [35] Lebedev A V 2013 *Colloid J.* **75** 386–390
- [36] Allen M P and Tildesley D J 1987 *Computer simulation of liquids* (Oxford: Clarendon Press)
- [37] Elfimova E and Ivanov A 2008 *Magnetohydrodynamics* **44** 39–44
- [38] Elfimova E A and Ivanov A O 2010 *J. Exp. Theor. Phys.* **111** 146–156